A GPR Survey of Arctic Pingos

John H Bradford
Dept. of Geophysics
Colorado School of Mines
Golden, Colorado, USA
jbradford@mines.edu,

Benjamin Hills
Dept. of Geophysics
Colorado School of Mines
Golden, Colorado, USA
Benjamin.Hills@mines.edu

Roger Michaelides
Dept. of Earth, Environmental and Planetary Sciences
Washington University
St. Louis, MO, USA
roger.michaelides@wustl.edu

Matthew Siegfried
Dept. of Geophysics
Colorado School of Mines
Golden, Colorado, USA
siegfried@mines.edu

Venezia Follingstad
Dept. of Geophysics
Colorado School of Mines
Golden, Colorado, USA
vfolling@uoregon.edu

Kynan Hughson
Dept. of Earth Sciences
University of New Brunswick
Fredericton, Canada
kynan.hughson@unb.ca

***Abstract*—The Pingo STARR project has undertaken a large geophysical study of Arctic pingos designed to investigate their internal structure and evolution over time. GPR surveys of thirteen pingos reveal significant variability of internal architecture despite similarities in surface morphology. Of the thirteen pingos, only two show evidence of the well-developed massive ice core that is predicted by the classic model of pingo formation. These results call for a new, more nuanced approach to understanding pingo formation and evolution.**

Keywords—depth imaging, pingo, permafrost

I. Introduction

Pingos are-ice cored mounds that form in permafrost terrain on Earth, and are indicative of intrapermafrost hydrologic systems. They are classified as either hydrostatic that are formed from a closed water source such as a thermokarst basin, or hydraulic that are formed from an open groundwater source [1][2]. All of the pingos surveyed in this study are classified as hydrostatic. Similar topographic features have been observed on extraterrestrial systems such as Mars and Ceres [3][4]. The Pingo SubTerranean Aquifer Reconnaissance and Reconstruction (Pingo STARR) project is designed to investigate the evolution of pingos over time. The investigation will lead to improved understanding pingo formation which may be a helpful analog for future space exploration.

In the conceptual model of pingo formation, early stages of growth are characterized by water intruding from below, spreading laterally along permeable strata, then refreezing and forming impermeable boundaries. In this model, water continues to intrude and refreeze, underplating previously formed ice lenses. Over time, a well-defined, massive ice core forms. When the water source is depleted, the pingo degrades as the ice core collapses. The collapse may leave stranded massive ice volumes separated by faults and interspersed with discontinuous soil.

While prior reports of the use of ground-penetrating radar (GPR) to study pingos are rare, it is not unprecedented. For example, Ross et al. [5] used GPR to study open system pingos on Svalbard. The Ping STARR project is the most comprehensive geophysical investigation of pingos yet reported. Over the course of three field seasons, we have surveyed thirteen different pingos using ground-penetrating radar (GPR), capacitively coupled resistivity (CCR), and time-domain electromagnetic (TEM) measurements [6]. Of these pingos, four are located inland on the North Slope of Alaska near Prudhoe Bay [7], and likely formed from a fresh water source. The remaining nine are coastal pingos located in the Canadian Pingo Landmark, Northwest Territories, Canada. These pingos likely formed in a brackish environment. The pingos vary in height from 6 m to nearly 50 m. The pingos exhibit a range of surface morphology that include: 1) low broad mounds that are potentially in early stage development, 2) well-formed conical structures with fully developed morphology, and 3) degraded or collapsed structures. By imaging internal pingo structure at different stages of development, our intent is to better understand architecture throughout the lifecycle.

Of the thirteen pingos surveyed, nine have the classic surface morphology associated with a mature pingo, yet only two of these display evidence of a well-defined, massive ice core. In general, the internal structures are highly variable despite surface appearance. This observation challenges the classic conceptual model of pingo formation and calls for a more nuanced understanding of pingo growth. Here we describe and compare observations from six pingos, three from Alaska and three from Canada.

II. Field Site Descriptions

A. North Slope, Alaska

The Alaskan pingos are located roughly 50 km inland from Prudhoe Bay, and vary in height from 6 m to 19 m. The morphologies range from low lying and immature to fully formed, sub-conical structures, and were formed from fresh groundwater. Here we discuss three specific pingos. Pingo 8, at just over 12 m high, is characterized by classic conical pingo morphology (Figure 1A). Pingo 7, at nearly 19 m high, also displays classic pingo surface morphology (Figure 1C) and Pingo 9 (Figure 1E), with low lying broad topography, is considered immature.

B. Pingo Canadian Landmark

The Pingo Canadian Landmark is located on the coast, east of the of Mackenzie River Delta, in the northern Northwest Territories, Canada. It contains an exceptionally high concentration of pingos including the world's second tallest

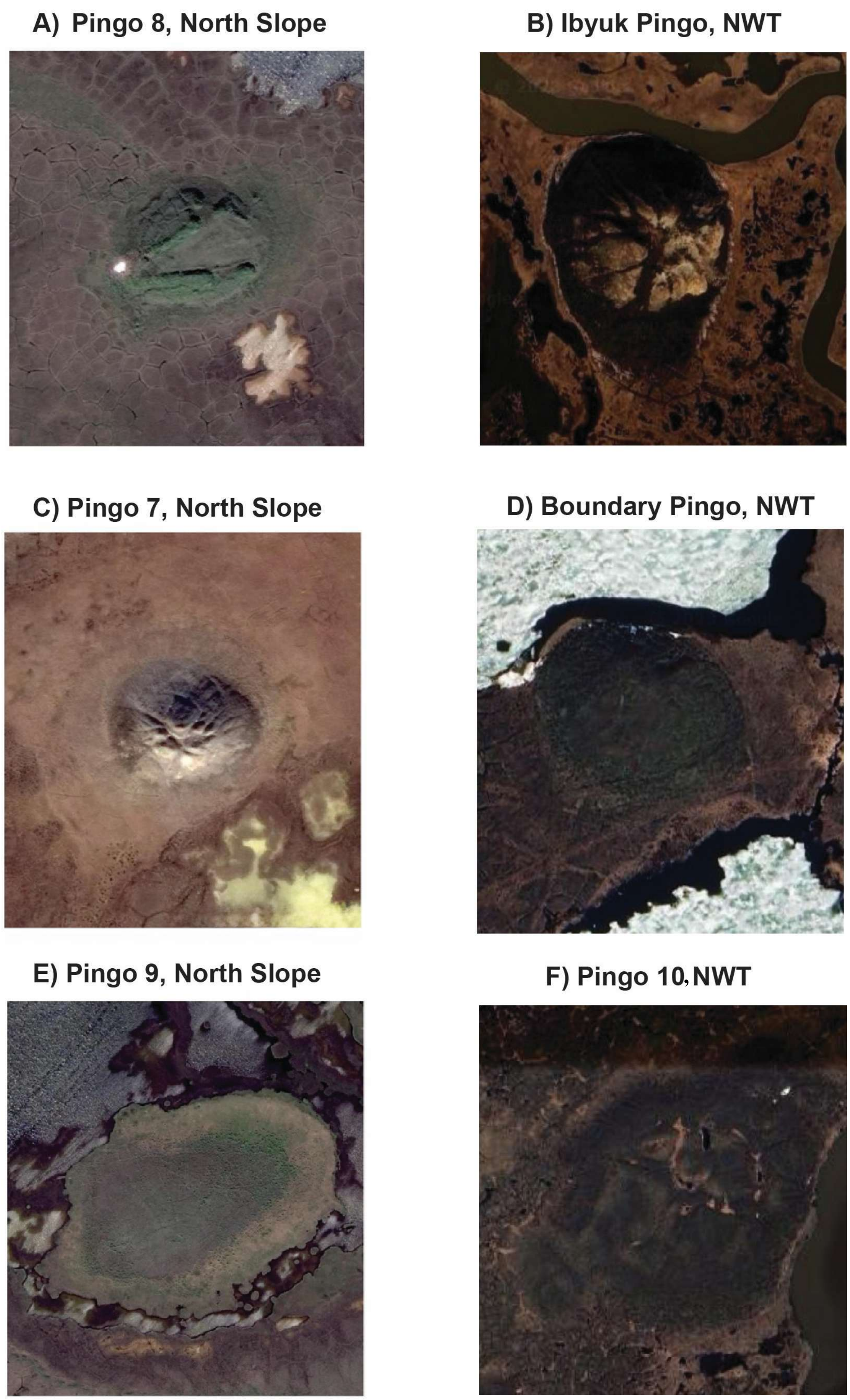

Figure 1. Google Earth images of pingos on the Alaskan North Slope (A, C, and E) compared to similar pingos in the Pingo Canadian Landmark (B, D, and F). A-D show the expected surface topography of a mature pingo, yet only A and B show evidence of a developed ice core. E and F are broad, low pingos, but differ significantly in internal structure.

pingo, Ibyuk Pingo, at over 50 m high. Ibyuk is a type defining pingo with well-defined conical surface morphology (Figure 1B). We include two additional Canadian pingos in this discussion. Boundary Pingo (Figure 1D) has classic pingo morphology and is similar in size to North Slope Pingo 7. Pingo 10 (Figure 1F) is a low lying broad pingo similar in size and morphology to North Slope Pingo 9. The Canadian pingos are on the coast with several pingos surrounded by the brackish shallow waters of a small bay, and likely have formed from saline water. Formation of ice from saline water differs from fresh water ice due to expulsion of salts during crystal formation accompanied by entrainment of highly concentrated brines in the interstitial spaces. Retention of highly concentrated liquid brine in saline ice increases ice conductivity, as well as altering the mechanical properties.

III. GPR Data Acquisition and Processing

At all sites, 2D data were acquired under winter conditions with frozen ground and firm, wind-packed snow on the surface. A studded survey wheel was used to trigger the radar at regular intervals.

Data at the Alaskan pingos were acquired with a Sensors and Software Spidar multi-channel system with 50 MHz, and 100 MHz antennas with nominal 0.50 m and 0.25 m trace spacing respectively. Absolute position control was maintained with a roving GPS antenna affixed to the snow machine that was towing the radar antenna sled. Differential post processing indicates elevation uncertainty of less than 10 cm. The antenna frequency profiles selected for this exposition best illustrate the key comparative points.

Data at the Canadian pingos were acquired in single offset mode with 50 MHz antennas and the Sensors and Software ultra-receiver, with a nominal 0.25 m trace spacing. Due to the rugged topography, a hand pulley system was utilized to move the radar system up and over the pingos with the GPS positioning antenna affixed to the radar sled. Note that the south face of Ibyuk Pingo was too steep to acquire data safely and only the northern portion of the pingo was surveyed. Trace stacking and spacing were optimized considering signal to noise ratio, data density, and rate of data acquisition. The number of stacked traces varies from 4096 to 8192, and the signal to noise ratio is significantly improved compared to repeat profiles using the previous generation radar system that we deployed in Alaska. Increased conductivity in the Canadian pingos was confirmed by capacitively coupled resistivity surveys [6] and the Canadian GPR profiles are characterized by significantly greater attenuation, particularly in zones outside of the cores of the pingos.

The following data processing steps were applied to all data: 1) time-zero correction, 2) DEWOW, 3) low pass time domain filter, 4) exponential gain correction. Additionally, all profiles have been 2D depth migrated from topography using the reverse-time migration algorithm described by Bradford [8].

IV. GPR Results

Of the thirteen pingos surveyed, only North Slope Pingo 8 (Figure 2A) and Ibyuk Pingo (Figure 2B) show evidence of a well-defined, massive ice core. The image of Pingo 8 is remarkable for its near ideal internal structure. The top of the ice core mimics the surface topography, while the base of the ice is flat and at an elevation similar to the surrounding topography. Deformed, uplifted soil stratigraphy is present along the flanks of the pingo. The massive ice core present in Ibyuk Pingo occupies proportionally less of the interior of the pingo than Pingo 8. Further, while the upper surface of the ice core is surface mimicking, the ice core is lenticular rather than flat bottomed, with the deepest part of the ice lense extending below the surrounding ground surface. There is some evidence of ice deformation, which potentially indicates the early stages of pingo collapse.

While Pingo 7 (Figure 2C) and Boundary Pingo (Figure 2D) both illustrate the classic pingo surface morphology, the interior structure is not consistent with the standard conceptual model of pingo formation. Neither pingo shows evidence of a well-defined ice core, but both pingos contain interior reflectors that are consistent with lateral ice lenses that have limited vertical extent. Boundary Pingo does contain a relatively small lenticular feature, 5 - 10 m below the surrounding ground surface, with a lateral extent of approximately 20 m. Based on initial polarization analysis we interpret this lens as a massive ice structure, and speculate that it may be in its early phase of formation.

North Slope Pingo 9 (Figure 2E) and Canadian Pingo 10 (Figure 2F) both exhibit low lying broad topographic relief but differ significantly in their dominant internal structure. The GPR texture of Pingo 9 lacks well defined coherence: it is defined by chaotic reflectivity. However, there is a high amplitude, but irregular reflection present at a depth of > 20 m; significantly below the ground surface. Given the high reflectivity of this feature, it may be the upper surface of a broad talik that is the fresh water source for pingo formation. Pingo 10 is characterized by three prominent scattering features. These scattering features correlate with ice wedges observed on the surface. The ice wedges appear to extend to 6-7 m below the top of the pingo, and likely contain low conductivity fresh water ice formed from snow melt and rain water accumulation. The high amplitude reflectivity suggests liquid water at the base of the ice wedges. The ice wedges form low conductivity, high velocity, vertical wave guides that enable radar wave propagation with little attenuation. The interior of Pingo 10 between the ice wedges is nearly transparent. Correlation with electrical resistivity data (not presented here) indicates elevated conductivity in the intrawedge space. High radar attenuation is the likely explanation for lack of reflectivity, rather than lack of the subsurface structure.

V. Discussion

Generally, and not surprisingly, GPR is an excellent tool for interrogating the interior structure of pingos. Antennas in the frequency range of 50 MHz to 100 MHz provide a nice balance of depth of penetration and resolution for both freshwater and coastal pingos.

The Pingo STARR project is the most extensive geophysical study of pingo interior structure to date. Of the thirteen pingos investigated thus far, only two show evidence of the well-defined massive ice core that is central to the classic model of pingo formation. Our results clearly indicate that the classic model of pingo genesis and evolution need to be revisited.

Acknowledgment

This work is supported by NASA PSTAR Grant 80NSSC20K1133. Grant PI Britney Schmidt, along with team members Tyler M. Meng, Alexia Kubas, Andrew Mullen

Enrica Quartini, Austin Routt, Hanna Sizemore, and Andrei Swidinsky were instrumental to project development and contributed significantly to data acquisition.

References

[1] J.R. Mackay, “The growth of pingos, Western Arctic Coast, Canada,” 1973, Can. J. Earth Sci., pp. 979-1004.

[2] J.R. Mackay, “Pingo growth and collapse, Tuktoyaktuk Peninsula Area, Western Arctic Coast, Canada: a long-term field study,” 1998, Géog. phys. Quat., pp. 271-323.

[3] D.M. Burr, K.L. Tanaka, K. Yoshikawa, “Pingos on Earth and Mars,” 2009, Plan. and Sp. Sci., pp. 541-555.

[4] B. E. Schmidt, H. G. Sizemore, K. H. G. Hughson, K. D. Duarte, V. N. Romero, J. E. C. Scully, P. M. Schenk, D. L. Buczkowski, D. A. Williams, A. Nathues, K. Udell, J. C. Castillo-Rogez, C. A. Raymond, C. T. Russell, “Post-impact cryo-hydrologic formation of small mounds and hills in Ceres’s Occator crater,” 2020, Nat. Geosci., pp. 605–610.

[5] N. Ross, C. Harris, H.H., Christiansen, P.J. Brabham, “Ground penetrating radar investigations of open system pingos, Adventdalen, Svalbard,” 2005, Nor. J. Geog., pp.129-138.

[6] K. Hughson, B. Schmidt, M. Siegfried, J. Bradford, A. Kubas, A. Routt, et al., “High variability observed in the internal structure of arctic pingos: implications for hydrologically derived icy landforms across the solar system,” Abstract EP53A-1456, 2024 Fall Meeting, AGU, Washington, DC, December 2024.

[7] J. Bradford, M. Siegfried, V. Follingstad, K. Hughson, A. Routt, B. Schmidt, et al., “Mapping the internal structure of Arctic pingos using ground-penetrating radar,” 2024, Proc. 2023 Intl. Conf. Eng. Geoph., Al Ain, UAE.

[8] J. Bradford, J. Rozar, D. Wilkins, and R. Ford, “Reverse time migration from rugged topography to image ground-penetrating radar data in complex environments,” 2018, Eng., pp. 661-666.

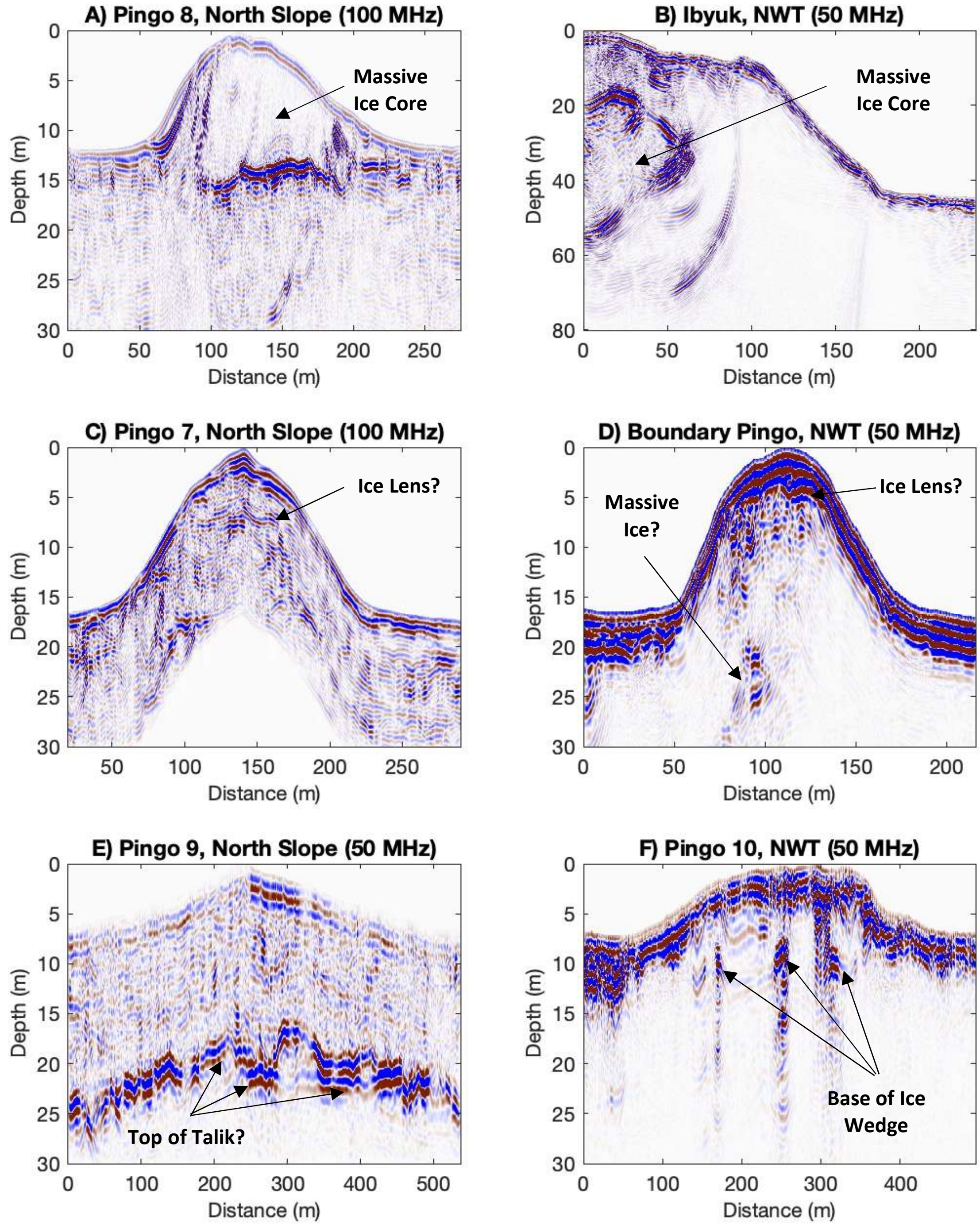

Figure 2. Reverse Time Migrated images on the Alaskan North Slope (A, C, and E) compared to similar pingos in the Pingo Canadian Landmark (B, D, and F). Pingo 8 (A), displays classic pingo architecture with a well-developed ice core that mimics surface topography on top, but has a flat bottom just below the surrounding elevation. Ibyuk Pingo (B) also has a large, well developed ice core, but it has lenticular geometry. No other pingos have evidence for a large ice core. C and D contain apparent ice lenses, and D may have a small massive ice core. The young pingos, E and F, are different in structure, but neither displays a coherent internal structure.